EV20-sss-vc/MMAF, an HER-3 targeting antibody-drug conjugate displays antitumor activity in liver cancer

DANIELA D'AGOSTINO[1,2*], ROBERTA GENTILE[3,4*], SARA PONZIANI[3,4], GIULIA DI VITTORIO[3,4],
FRANCESCO DITURI[5], GIANLUIGI GIANNELLI[5], COSMO ROSSI[2], LIBERATO MARZULLO[6],
FRANCESCO GIANSANTI[3], VINCENZO DE LAURENZI[1,2], STEFANO IACOBELLI[4],
RODOLFO IPPOLITI[3], EMILY CAPONE[1,2] and GIANLUCA SALA[1,2]

[1]Department of Medical, Oral and Biotechnological Sciences, University of Chieti-Pescara 'G. D'Annunzio';
[2]Center for Advanced Studies and Technology (CAST), I-66100 Chieti; [3]Department of Life,
Health and Environmental Sciences, University of L'Aquila, I-67100 Coppito; [4]MediaPharma SRL, I-66100 Chieti;
[5]National Institute of Gastroenterology 'S. de Bellis' Research Hospital, Castellana Grotte, I-70013 Bari;
[6]Department of Medicine, Surgery and Dentistry 'Scuola Medica Salernitana',
University of Salerno, I-84081 Baronissi (SA), Italy

Abstract. Liver cancer (LC) is an aggressive disease with a markedly poor prognosis. Therapeutic options are limited, and, until recently the only FDA-approved agent for first-line treatment of patients with LC was the multi-kinase inhibitor sorafenib, which exhibits limited activity and an increased overall survival (OS) of only 3 months over placebo. Therefore, the development of alternative therapeutic molecules for the treatment of LC is an urgent medical need. Antibody-drug conjugates (ADCs) are an emerging class of novel anticancer agents, which have been developed recently for the treatment of malignant conditions, including LC, and are being studied in preclinical and clinical settings. Our group has recently generated an ADC [EV20/monomethyl auristatin F (MMAF)] by coupling the HER3 targeting antibody (EV20) to MMAF via a non-cleavable maleimidocaproyl linker. This ADC was revealed to possess potent therapeutic activity in melanoma and breast carcinoma. In the present study, using western blot and flow cytometric analysis, it was reported that HER-3 receptor was highly expressed in LC and activated by its ligand NRG-1β in a panel of LC cell lines, thus indicating that this receptor may serve as a suitable target for ADC therapy. A novel ADC [EV20-sss-valine-citrulline (vc)/MMAF] was generated, in which the cytotoxic payload MMAF was site-specifically coupled to an engineered variant of EV20 via a vc cleavable linker. Cytotoxicity assays were performed to investigate *in vitro* antitumor activity of EV20-sss-vc/MMAF and it was compared to EV20/MMAF, which revealed only modest activity in LC.EV20-sss-vc/MMAF exhibited a significant cell killing activity in several LC cell lines. Additionally, *in vivo* xenograft experiments revealed that EV20-sss-vc/MMAF inhibited growth of LC tumors. The present data indicated that EV20-sss-vc/MMAF is a worthy candidate for the treatment of HER-3 positive LC.

Introduction

Liver cancer (LC) is an aggressive disease with high mortality rate (1). Despite the considerable efforts made in recent years to increase the therapeutic arsenal against LC, an efficient cure for advanced LC continues to be an unmet medical need. In fact, prognosis for patients with advanced LC remains markedly poor, with a mean survival estimated between 6 and 20 months (2-5). The limited response to therapies observed in LC patients, is mainly due to the resistance of tumor cells to chemotherapeutic substances (6). Sorafenib, a multiple kinase inhibitor, FDA-approved since 2007 has exhibited some limited survival benefits (7-9). However, the majority of LC patients do not respond to sorafenib and most of initially responsive patients, subsequently become refractory to this agent (10). A recent study demonstrated that signaling pathways controlled by EGFR and HER-3 restrict sorafenib effects both in naïve and sorafenib-resistant LC (11). In fact, it has been proposed that combination of sorafenib with EGFR inhibitor gefitinib may increase anti-proliferative response and prevent resistance in LC cellular models.

HER-3 belongs to the ERBB receptor family, which includes the epidermal growth factor receptor (EGFR) also

Correspondence to: Dr Gianluca Sala or Dr Emily Capone, Department of Medical, Oral and Biotechnological Sciences, University of Chieti-Pescara 'G. D'Annunzio', Via dei Polacchi 11, I-66100 Chieti, Italy
E-mail: g.sala@unich.it
E-mail: emily.capone@unich.it

*Contributed equally

known as HER1, ERBB2/HER2/Neu, and ERBB4/HER4. These tyrosine kinase receptors are aberrantly activated in multiple cancers and therefore serve as drug targets and biomarkers in targeted therapy (12). The therapeutic potential of HER-3 has been underestimated for a long time, mainly due to its low kinase activity; however, a large body of evidence has been collected in recent years revealing a prime role for this receptor in modulating the sensitivity of targeted therapeutics in several cancers.

In fact, compensatory upregulation of HER-3 expression and downstream phosphatidylinositol 3-kinase (PI3K)/AKT signaling is considered as one of the most common mechanisms used by tumor cells to evade the blockade promoted by targeted therapy (as gefitinib in lung cancer, PI3K inhibitors in breast cancer, RAF/MEK inhibitors in melanoma) (12-14). Moreover, HER-3 somatic oncogenic mutations have been described in a significant proportion of gastric and colon cancer patients (15). Therefore, a considerable effort has recently been made on the development of drugs able to block the activity of this receptor. In particular, several naked antibodies have been tested in clinical stages both as mono-therapy and in combination with several approved anticancer drugs (13,16). However, results from these studies were not satisfactory.

Recently, the use of antibody-drug conjugates (ADCs) has emerged as an efficient therapeutic approach to target HER-3-positive tumor cells. ADCs are an attracting class of novel anticancer agents in the field of precision oncology, which preclinical and clinical development has been of increased interest for the treatment of several tumors, including LC (17-19).

We have previously provided evidence that EV20/monomethyl auristatin F (MMAF), an ADC generated by coupling the HER3 targeting antibody EV20 (20-23) to MMAF via a non-cleavable maleimidocaproyl linker possesses potent and specific therapeutic activity in melanoma (24) and breast carcinoma (25).

In the present study, we developed a novel anti-HER-3 targeting ADC [named EV20-sss-valine-citrulline (vc)/MMAF] by site-specific conjugation of an engineered variant of EV20 to MMAF via a vc cleavable linker. The antitumor efficacy of EV20-sss-vc/MMAF was investigated using *in vitro* and *in vivo* approaches.

Materials and methods

Reagents. Antibodies used in the present study were as follows: phosphorylated (p)-ErbB-3 (Tyr1289; clone 21D3; product no. 4791), ErbB-3 (clone D22C5; product no. 12708), p-EGFR (Tyr1068; clone D7A5; product no. 3777), EGFR (clone D38B1; product no. 4267), GAPDH (clone D16H11; product no. 5174), p-Akt (Ser473; clone D9E; product no. 4060), Akt (product no. 9272), p-Erk1/2 (Thr202/Tyr204; clone D.13.14.4E; product no. 4370), Erk1/2 (clone 137F5; product no. 4695), all from Cell Signaling Technology, Inc.; and anti-β-actin (product no. A5441) was purchased from Sigma-Aldrich; Merck KGaA. Neuregulin-1β (NRG-1β; product no. 5218SC) was purchased Cell Signaling Technology, Inc. Recombinant human EGF (cat. no. AF-100-15) was purchased from ProSpec-Tany TechnoGene Ltd. EV20 antibody was produced as previously described (22,23). Free MMAF (cat. no. HY-15579A)

and sorafenib (cat. no. HY-10201) were purchased from MedChemExpress. The multidrug resistance-associated protein inhibitors PSC833 (CAS no. 121584-18-7; product no. SML0572), Reversan (CAS no. 313397-13-6; product no. SML0173) and MK571 (CAS no. 115104-28-4; product no. MK-571), used in combination with free MMAF in the MTT assay, were purchased from Sigma-Aldrich; Merck KGaA. T-DM1 was kindly provided by Professor Atanasio Pandiella from Centro De Investigaciòn del Càncer (Barcelona, Spain).

Cell lines. A375m human melanoma cell line (CRL3223) and SJSA-1 human osteosarcoma cell line (CRL2098) were purchased from ATCC. Liver cancer cell lines (HepG2, Hep3B, HuH7, SNU449, and PLC/PRF/5) were kindly provided by Dr Dituri Francesco from the National Institute of Gastroenterology 'S. de Bellis' Research Hospital (Castellana Grotte, Bari, Italy). HepG2 cells were authenticated by ATCC using Short Tandem Repeat (STR) DNA analysis. HepG2SR cells were obtained from culturing HepG2 parental cells in the presence of increasing doses of sorafenib up to a final concentration of $2\,\mu M$. All cell lines were cultured less than 3 months after resuscitation. The cells were cultured according to manufacturer's instructions, using EMEM for HepG2, Hep3B and PLC/PRF/5 cells, DMEM for HuH7 and A375m cells, and RPMI-1640 medium (all from Thermo Fisher Scientific, Inc.) for SNU449 and SJSA-1 cells, supplemented with 10% heat-inactivated fetal bovine serum (FBS; Invitrogen; Thermo Fisher Scientific, Inc.), L-glutamine, 100 U/ml penicillin, and $100\,\mu g/ml$ streptomycin (Sigma-Aldrich; Merck KGaA), and incubated at 37°C in humidified air with 5% CO_2.

Generation of EV20-based antibody-drug conjugates. EV20/MMAF was generated by Levena Biopharma (http://www.levenabiopharma.com/) as previously described (24,25). For site-specific conjugation, EV20 was engineered to EV20-sss as previously reported (26). Briefly, the cysteine residues of the heavy chain in positions 220, 226 and 229 were mutated into serine. EV20-sss-vc/MMAF was obtained as follows: EV20-sss was reduced using 60 M excess of Tris(2-carboxyethyl)phosphine (TCEP; Thermo Fisher Scientific, Inc.) in phosphate-buffered saline (PBS; Sigma-Aldrich; Meck KGaA), pH 7.4. The reaction was carried out overnight at room temperature. The reaction was stopped by passing the EV20-sss/TCEP mixture through a PD10 column (Cytiva) equilibrated in PBS, pH 7.4. The reduced antibody was then reacted with 10 M excess of MMAFvc in PBS overnight at room temperature. The reaction was stopped by adding 500-fold molar excess iodoacetamide (Sigma-Aldrich; Merck KGaA). To eliminate unreacted free auristatin, the reaction mixture was passed through a G25 Sephadex column equilibrated in PBS/5% sucrose/10% DMA in an isocratic way with a flow rate of 1 ml/min. The final concentration of the ADCs was estimated by UV-VIS spectrophotometry, using an extinction coefficient $\varepsilon 280 = 1.5\,M^{-1}\,cm^{-1}$. The auristatin MMAFvc was provided by Levena Biopharma (http://www.levenabiopharma.com/). To evaluate the drug antibody ratio (DAR), hydrophobic chromatography (HIC)-HPLC was performed on conjugated and unconjugated antibody sample, dialyzed in solution containing 1.5 ammonium sulphate, 50 mM sodium phosphate, isopropanol 5%, pH 7.

Subsequently, both samples (0.3 mg/ml) were analyzed in HIC-HPLC (Sol.A: 1.5 ammonium sulphate, 50 mM sodium phosphate, isopropanol 5%, pH 7; Sol.B: 50 mM sodium phosphate, isopropanol 20%, pH 7) with gradient 0-100% Sol.B in 20 min, flow rate 1 ml/min.

Flow cytometric analysis. For HER receptors surface expression analysis, flow cytometry was performed as follows. Approximately one million growing cells were harvested and labeled with 1 μg/ml of primary antibody for 30 min on ice. For EGFR, HER-2 and HER-3 staining, primary antibodies used were chimeric anti-EGFR cetuximab (cat. no. A2000), humanized anti-HER-2 trastuzumab (cat. no. A2007), both purchased from Selleck Chemicals, and EV20 (humanized anti-HER-3, developed in our laboratory (Mediapharma srl, University of Chieti-Pescara, Chieti, Italy) (22,23). All primary antibodies were used at the dilution of 1 μg/1x10^6 cells. After washing, the cells were labelled with PE-conjugated goat anti-Human Fc as secondary antibody at a dilution of 1:300 (cat. no. H10104; Molecular Probes; Life Technologies; Thermo Fisher Scientific, Inc.) for 30 min on ice. Regarding HER-4 analysis, cells were fixed with 1% paraformaldehyde for 15 min at room temperature and permeabilized with 0,1% Triton X-100 for 5 min at room temperature, then stained for 30 min on ice with 1 μg/ml of anti-HER4 antibody (cat. no. MA1-861; Invitrogen; Thermo Fisher Scientific, Inc.) as a primary antibody followed by staining for 30 min on ice with goat anti-mouse IgG Alexa-Fluor 488-conjugated at a dilution of 1:300 (cat. no. A11001; Molecular Probes, Life Technologies; Thermo Fisher Scientific, Inc.). For the *in vivo* binding assay of EV20 and EV20-based ADCs, A375m cells were detached and labelled with 10 μg/ml of EV20 and EV20-sss-vc/MMAF for 30 min on ice, followed by staining for 30 min on ice with PE-conjugate goat anti-Human Fc as a secondary antibody at a dilution of 1:300 (cat. no. H10104). Analysis was performed using FACSCantoII cytometer (BD Biosciences). Data were analyzed with FlowJo software V10.7 (FlowJo, LLC).

Cytotoxicity assays. Cell proliferation was assessed by 3-(4,5-dimethyldiazol-2-yl)-2,5-diphenyl tetrazolium bromide (MTT) assay (Sigma-Aldrich; Merck KGaA). Cell lines were seeded into 24-well plates at a density ranging between 4x10^3 cells/well and 7x10^3 cells/well in 500 μl of complete culture medium. Then, cells were treated with drugs at indicated concentrations in triplicates and further incubated for 120 h. At the end of the incubation period, cells were incubated with 200 μl of MTT solution (serum-free medium with 0.5 mg/ml of MTT) for a further 2 h. After removal of MTT solution, 200 μl of dimethyl sulfoxide (DMSO) was added to the wells for 10 min and the absorption value at 570 nm was measured using a multi-plate reader. All experiments were performed in triplicate and the IC$_{50}$ values were calculated using GraphPad Prism 5.0 software (GraphPad Software, Inc.).

Western Blotting. Lysates from cells in culture were prepared by washing cells twice in cold PBS followed by lysis with RIPA Buffer (50 mM Tris-HCl, 1% NP-40, 0.1% SDS, 150 mM NaCl) supplemented with protease and phosphatase inhibitors (Sigma-Aldrich: Merck KGaA) for 10 min at 4°C. Insoluble materials were removed by centrifugation (16,000 x g for

10 min at 4°C) and protein concentration was assessed using a Bradford assay. Equal amounts of protein (30 μg) were separated by SDS/PAGE on 10% polyacrylamide gel and transferred to nitrocellulose membranes. Membranes were blocked with 5% non-fat dry milk in PBS containing 0.1% Tween-20 for 1 h at room temperature and incubated with following primary antibodies: p-ErbB-3, ErbB-3, p-EGFR, EGFR, p-Akt, Akt, p-Erk1/2, Erk1/2, all from Cell Signaling Technology, Inc. and anti-β-actin from Sigma-Aldrich; Merck KGaA, as aforementioned. All the antibodies were used at a dilution of 1:1,000 in PBS containing 0.1% Tween-20 overnight at 4°C, except for anti-β-actin, which was used at a dilution of 1:40,000 in PBS containing 0.1% Tween-20. After washing, the membranes were hybridized for 1 h at room temperature with horseradish peroxidase-conjugated secondary antibodies at a dilution of 1:20,000 [(HRP-conjugated goat anti-mouse IgG; product code STAR207P) and (HRP-conjugated goat anti-rabbit IgG; product code STAR208P; both purchased from Bio-Rad Laboratories, Inc.]. Detection was performed with Plus-ECL chemiluminescence kit (Bio-Rad Laboratories, Inc.). Densitometric analysis of bands was performed using ImageJ software V1.53 (National Institutes of Health).

HER-3 expression in tumor and peritumor samples. For the evaluation of HER-3 protein expression in human specimens, tumor and peritumor samples, as well as normal liver samples, were collected, snap-frozen, and analyzed by western blotting. Male (n=9) and female (n=2) patients aged between 48 and 80 years were included. Samples were collected at the Department of Emergencies and Organ Transplant of the Policlinic Hospital of Bari (Bari, Italy), between September 2016 and September 2017. All patients provided written consent for the use of their specimens for research purposes; none were identifiable. Frozen specimens of tissues were homogenized with a Polytron homogenizer in a lysis buffer T-PER Tissue Protein Extraction (cat. no. 78510; Thermo Fisher Scientific, Inc.) supplemented with proteinases/phosphatases inhibitor cocktail (cat. no. 1861280; Thermo Fisher Scientific, Inc.). The homogenates were then centrifuged at 16,000 x g for 10 min at 4°C, and the protein concentration was determined using a Bio-Rad assay kit according to the manufacturer's instructions (cat. no. 131947; Bio-Rad Laboratories, Inc.). Equal amounts of proteins (20 μg) were separated by SDS/PAGE on 10% polyacrylamide gel and transferred to a nitrocellulose membrane. The membrane was probed overnight at 4°C with the HER-3 (product no. 12708) and GAPDH (product no. 5174; both 1:1000; both from Cell Signaling Technology, Inc.) antibodies, washed with TBS-T (TBS 1X + 0.05% Tween-20), and then incubated for 1 h at room temperature with horseradish peroxidase-conjugated secondary antibody (HRP-conjugated goat anti-rabbit IgG; cat. no. STAR208P; Bio-Rad Laboratories, Inc.) at the dilution of 1:20,000 in TBB buffer (TBS-T + 5% nonfat milk). Detection was performed with Clarity Max Western ECL Substrate (Bio-Rad Laboratories, Inc.). This study was approved by the Local Ethics Committee, Azienda Ospedaliero Universitaria Consorziale Policlinico di Bari (Bari, Italy); protocol no. 254; date of release, February 2012.

Internalization assays. For flow cytometric quantification, A375m and HepG2 cells were plated in 60 mm plates and

grown in DMEM containing 10% FBS, for 24 h. Cells were then incubated with 10 μg/ml of EV20 in complete medium on ice for 30 min before returning the plates in the incubator at 37˚C for 1 h, maintaining control cells on ice in the presence of the antibody. Finally, the cells were detached and stained with PE-conjugate goat anti-Human Fc at a dilution of 1:300 (cat. no. H10104) for 30 min on ice. Analysis was performed using FACSCantoII cytometer (BD Biosciences). Data were analyzed with FlowJo software V10.7 (FlowJo, LLC).

For confocal microscopy, A375m and HepG2 cells were seeded on round cover slips in 12-well plates to 70% confluence in complete medium for 24 h. Cells were then incubated with 10 μg/ml of EV20 in complete medium on ice for 30 min, after which they were then incubated again at 37˚C for 2 h. The antibody was washed away and the cells were fixed for 15 min at room temperature with 4% paraformaldehyde (pH 7.4). Cells were then permeabilized for 5 min at room temperature with 0.5% Triton X-100 and labeled with goat anti-human IgG Alexa-Fluor 488-conjugated at a dilution of 1:200 (cat. no. A11013; Molecular Probes, Life Technologies; Thermo Fisher Scientific, Inc.) and Draq5 (product no. 4084; Cell Signaling Technologies, Inc.) to visualize nuclei. Images were acquired at a magnification of x63 with a Zeiss LSM 510 meta-confocal microscope (Zeiss AG) using 488- and 633-nm lasers.

ELISA. Recombinant HER-3 extracellular domain (ECD) (cat. no. ER3-H5223; AcroBiosystems) (1 μg/ml) was pre-coated overnight at 4˚C on 96 well-plates NUNC Maxisorp modules. After blocking with 1% BSA in PBS for 1 h at room temperature, increasing concentrations (ranging between 0.05 nM and 6.6 nM) of EV20-sss or EV20-sss-vc/MMAF were incubated for 1 h at room temperature. After several washes with PBS + 0,05% Tween-20, a goat anti-human IgG-HRP solution at a dilution of 1:5,000 (product no. A0170; Sigma-Aldrich; Merck KGaA) was added to each well and incubated for 1 h at room temperature. After washing, stabilized chromogen was added to each well for at least 10 min in the dark, then the reaction was stopped with the addition of H_2SO_4 1N and the absorbance was read at 450 nm with an ELISA reader.

Animal studies. Homozygous Balb/c nu/nu athymic female mice (4-6-weeks old) were purchased from Charles River Laboratories and maintained at 22-24˚C and relative humidity (40-60%) under pathogen-limiting conditions as required. Cages, bedding, and food were autoclaved before use. Mice were provided with a standard diet and water *ad libitum* and acclimatized for 2 weeks before the start of the experiments. Housing and all procedures involving the mice were performed according to the protocol approved by the Institutional Animal Care and Use Committee of the Italian Ministry of Health (authorization no. 292/2017-PR).

Five million of exponentially growing HepG2 cells were implanted subcutaneously (s.c.) into the right flank of the mice in a ratio of 1:6 with Matrigel (Cultrex Basement Membrane Matrix; cat. no. 3432-001-01; Trevigen, Inc.). When tumors became palpable (approximately 150 mm³), animals were randomly divided into two groups and treated intravenously via tail vein with vehicle (PBS, once a week for a total of 4 injections), or EV20-sss-vc/MMAF (10 mg/kg, once a week for a total of 4 injections), respectively. The tumor volume was monitored weekly by a caliper and calculated using the following formula: tumor volume (mm³) = (length x width²)/2. A tumor volume of 1.5 cm³ was selected as the endpoint for all experiments after which mice were sacrificed using CO_2 inhalation (20-70%).

Statistical analysis. For *in vivo* xenograft curves and HER-3 expression level in tumor tissues, P-values were determined by a paired Student's t-test and considered significant for P<0.05. Statistical analysis of PI3K/AKT activation was performed using one-way ANOVA, followed by Tukey's multiple comparisons test. Experimental sample numbers (n) are indicated in the figure legends. All statistical analysis was performed with GraphPad Prism 5.0 software (GraphPad Software, Inc.). Survival curves were evaluated by Kaplan-Meier and analyzed by the log-rank test with GraphPad Prism 5.0 software (GraphPad Software, Inc.).

Results

HER expression and signaling pathway in human LC. A panel of human LC cell lines for surface expression of HER-3 and its preferred partner HER-2 were screened by flow cytometry. The HER-3 and HER-2 receptors were expressed in all the LC cell lines assessed except for SNU449 cells, where HER-3 expression was found to be markedly low (Fig. 1A and B). Next, whether the downstream signalling of HER-3 was activated in these cells was evaluated. To this end, western blot analysis was performed of lysates prepared from this panel of LC cells stimulated with either HER-3 ligand neuregulin1b (NRG-1b) or epidermal growth factor (EGF), the ligand for the other member of the receptor family, EGFR. Notably, despite the fact that EGFR was highly expressed in this panel of cell lines (Fig. 1A), NRG-1b activated the PI3K/AKT the survival signaling pathway more potently than EGF (Fig. 1B). ERK activation was more pronounced upon NRG-1b stimulation in HepG2 cells. By contrast, a stronger activation upon EGF stimulation was observed in HuH7 and Hep3B cells, while PLC/PRF/5 and SNU449 exhibited high basal, but no inducible ERK phosphorylation (Fig. 1B).

Next, HER-3 receptor expression levels were evaluated by western blotting in 11 tumoral and corresponding peritumoral LC tissues. HER-3 expression was revealed to be significantly higher in tumoral than corresponding peritumoral tissues. Notably, HER-3 expression was barely detectable in normal liver tissues (Fig. 1C). All together these data indicated that HER-3 receptor was expressed in LC and that the NRG-1b/HER-3/Akt signalling axis was activated in these cancers, thus reinforcing the hypothesis that HER-3 may represent a suitable target for an ADC-based therapy.

Cytotoxic activity of EV20-based ADCs in LC cell lines. The antitumor activity of EV20/MMAF, an anti-HER-3 ADC, which we have recently revealed to possess a potent and specific therapeutic activity in melanoma and breast cancer models (24,25) was evaluated. Surprisingly, the activity of EV20/MMAF in LC cell lines was revealed to be significantly lower in comparison to the activity observed in non-LC cell
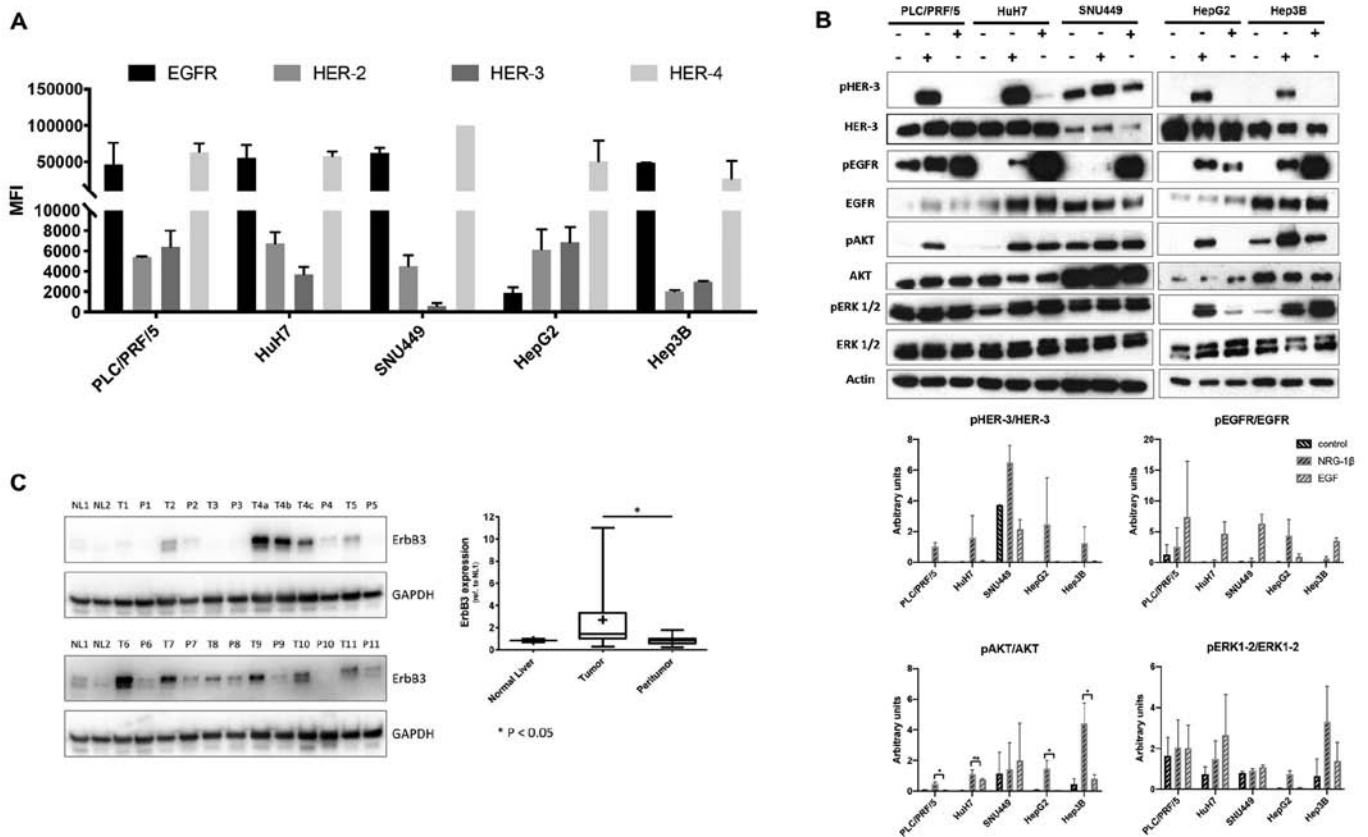
Figure 1. HER-3 is expressed and activated by NRG-1β in LC cells. (A) Surface expression of HER receptors was evaluated by flow cytometric analysis in a panel of LC cell lines. MFI ± SD (n=3). (B) LC cell lines were starved for 24 h and then stimulated with 10 ng/ml of NRG-1β or 20 ng/ml of EGF for 5 min. At the end of the incubation periods, cells were lysed and blotted with the indicated antibodies. The same membrane was reprobed with anti-actin antibody for a loading control. Densitometric analysis was performed using ImageJ software V1.53, and the means ± SD were expressed as arbitrary units. Statistical analysis of PI3K/AKT activation was performed using one-way ANOVA, followed by Tukey's multiple comparisons test (*P<0.05). (C) Lysates from tumor (T) and peritumoral (P) samples were analysed for HER-3 expression by western blotting. As control samples, NL tissues were used. Receptor expression was quantified and plotted on the right panel. The same membrane was reprobed with anti-GAPDH antibody for a loading control. MFI, mean fluorescence intensity; LC, liver cancer; NL, normal liver.

lines. In fact, IC_{50} values ranging between ~25 and ~70 nM were observed for HuH7 and PLC/PRF/5 cells, respectively, whereas an IC_{50} >100 nM was observed for the other three cell lines assessed (Fig. 2A).

To rule out the possibility that low efficacy of EV20/MMAF in LC cells was due to the impairment of an internalization process of the antibody/receptor complex, the EV20 internalization rate in HepG2 (LC, low responders) vs. A375m cells, which in our previous work were revealed to be markedly sensitive to this ADC (24), were compared. As revealed in Fig. 2B, no significant differences were observed between the two cell lines, indicating that the internalization process was functional in LC cells. Notably, HepG2 sensitivity to free MMAF was not significantly different from that of high-responder A375m melanoma cells (Fig. 2C, left panel) neither was it increased by multidrug resistance-associated protein inhibitors (such as Reversan, PSC833 and MK571 as reported in other systems (27,28) (Fig. 2C, right panel).

To improve the ADC activity, we generated a novel EV20-based ADC (named EV20-sss-vc/MMAF) maintaining the same cytotoxic payload coupled to an engineered variant of EV20 (named EV20-sss) generated by means of a cleavable linker, as described in the method section and in our previous work (26). The results obtained are presented in

HIC in Fig. 2D, by detecting at ε280 nm: with naked antibody (DAR =0) as a negative control, eluting with a retention time of 5 min, and present only in the sample of the unconjugated but not in the ADC chromatogram (0%); the antibody conjugated with DAR =1 is present in a small percentage (18%) (retention time 6 min); the antibody conjugated with DAR =2 is present at 7 min (82%). Percentages were obtained by integration of the peak area. Due to the site-specific conjugation process, this ADC had a fixed DAR of 2 or 1 (Fig. 2D). Moreover, EV20-sss-vc/MMAF was revealed to possess the same *in vitro* and cell binding ability of that observed with the naked EV20-sss (Fig. 2D) as well as receptor downregulatory capacity, while inhibition of ligand-induced HER-3 phosphorylation appeared slightly reduced in conjugated vs. naked EV20 antibody (Fig. 2E).

Notably, EV20-sss-vc/MMAF displayed higher cell killing activity than EV20/MMAF (Fig. 2A), although the two ADCs exhibited superimposable cell killing activity in A375m melanoma cells (Fig. 3A).

Additionally, EV20-sss-vc/MMAF cell killing activity was revealed to be to be strictly target-dependent. This was demonstrated by using HER-3 negative osteosarcoma SjSa-1cells, in which no cell killing could be observed (Fig. 3B) and by a competition assay with a 500-fold molar excess of naked
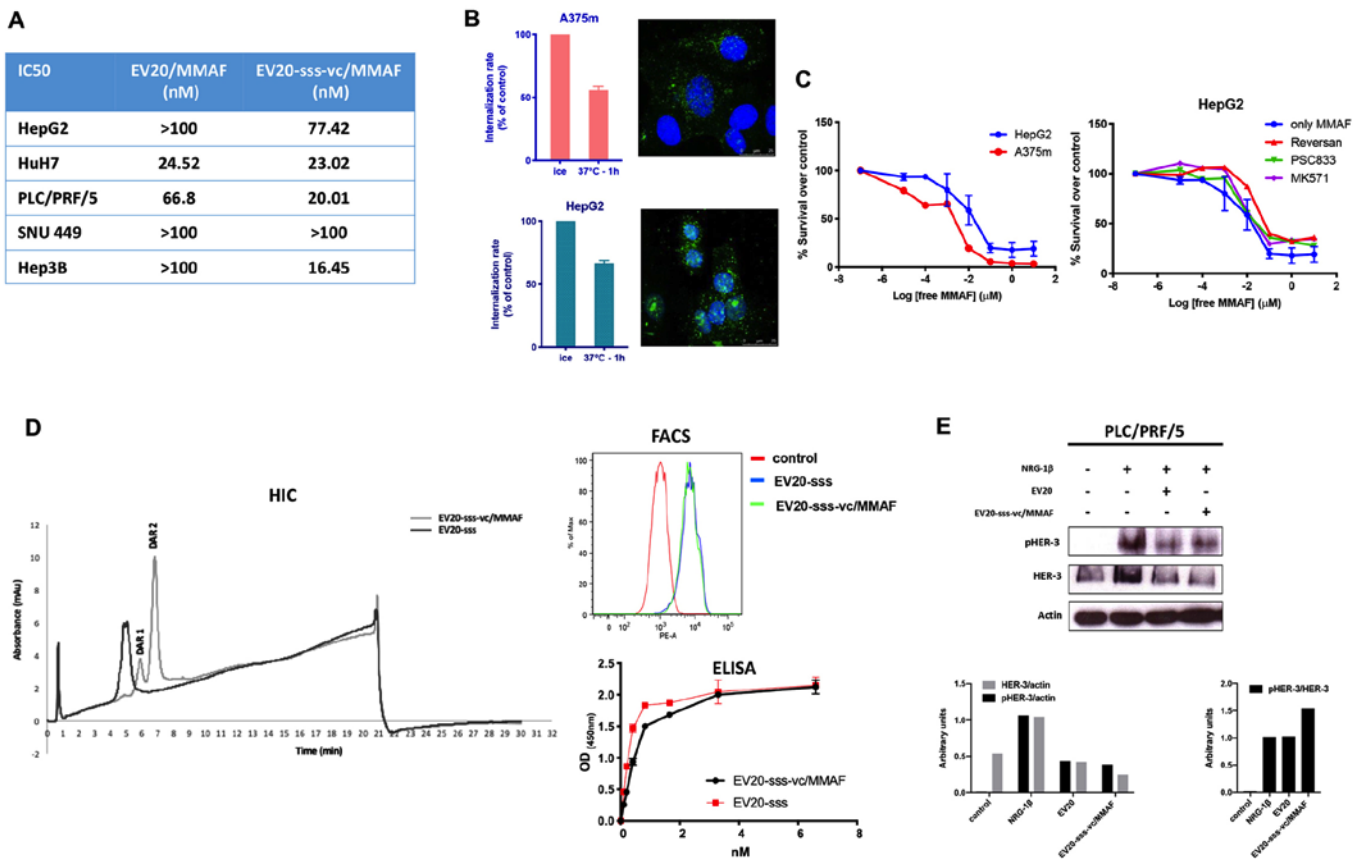
Figure 2. *In vitro* antitumor activity of EV20-based ADCs. (A) The cytotoxic response of LC cells to EV20-based ADCs treatment was evaluated by MTT after 120 h of treatment with increasing doses ranging between 0.006 nM and 100 nM. The IC_{50} values were calculated with GraphPad Prism 5.0 software and reported. (B) A375m and HepG2 cells were maintained for 30 min on ice in the presence of 10 μg/ml EV20 and placed again in the incubator at 37°C for 1 h. The internalization rate of the antibody was evaluated by flow cytometry and by confocal microscopy imaging. The histogram represents the percentage of MFI referred to control (cells maintained on ice). Plotted results are an average ± SD of three independent experiments. For confocal microscopy imaging, EV20 and nuclei were visualized on green and blue channels, respectively. (C) A375m and HepG2 cells were incubated for 72 h with eight increasing concentrations of free MMAF, diluted from 10 μM to 10 pM, in 1:10 dilution increments. Proliferation was evaluated by MTT assay (left panel). HepG2 cells were incubated for 72 h with the same increasing doses of free MMAF used in (C) in absence or presence of MK571 (25 μM), PSC833 (3 μM) and Reversan (15 μM) and proliferation was evaluated by MTT assay (right panel). (D) EV20-sss-vc/MMAF characterization. HIC was used for DAR calculation; melanoma A375m HER3+ cells were used for cell binding by flow cytometry. ELISA was performed for *in vitro* binding with naked EV20-sss mAb used as control. (E) PLC/PRF/5 LC cells were incubated for 2 h or not with naked or conjugated EV20 mAb, at a dose of 10 μg/ml, before NRG-1β stimulation (10 min, 10 ng/ml). Total and phosphorylated HER-3 receptor was analysed by western blotting and bands were quantified using actin as loading control. Histograms represent densitometric analysis of a single experiment, expressed as arbitrary units. MFI, mean fluorescence intensity; ADCs, antibody-drug conjugates; LC, liver cancer; MTT, 3-(4,5-dimethyldiazol-2-yl)-2,5-diphenyl tetrazolium bromide; MMAF, monomethyl auristatin F; vc, valine-citrulline; HIC, hydrophobic chromatography; DAR, drug antibody ratio.

EV20 antibody (Fig. 3C). Finally, the HER-3 low-expressing SNU 449 cells were revealed to be nearly insensitive to the ADC (Fig. 2A).

As HER-2 was revealed to be highly expressed in LC cells, the activity of EV20-sss-vc/MMAF was compared to the activity of the clinically approved anti-HER-2 ADC (T-DM1) in HepG2 cells. Despite the cells expressing similar levels of HER-2 and HER-3 (Fig. 1A), EV20-sss-vc/MMAF exhibited a significantly increased cell killing activity, suggesting this ADC was more effective in comparison to T-DM1 (Fig. 3D).

As HER-3 expression/activation is upregulated in response to several drugs, including sorafenib (11,20,29,30), it was investigated whether the activity of EV20-sss-vc/MMAF could be potentiated by combination with this agent. In line with a previous study (9), treatment of LC cells with sorafenib induced a potent cell killing activity with an IC_{50} ranging between ~7 and 1 μM (Fig. 4A, left panels). However, cell killing activity was not associated with the upregulation

of either HER-3 or HER-2 receptors (Fig. 4A, right panels). Similarly, no upregulation of HER-3 expression was detected in HepG2 cells grown under chronic exposure (up to 5 months) of 2 μM of sorafenib, (Fig. 4B, upper panel) and no increase of EV20-sss-vc/MMAF cell killing activity was observed in these cells (Fig. 4B, lower panel).

Antitumor activity in vivo. The therapeutic activity of EV20-sss-vc/MMAF ADC as a single agent in LC-derived xenografts was evaluated in xenografts assays. Although different methodological approaches were assessed, only mice harbouring tumours derived from subcutaneous injection of HepG2 were available for therapeutic study. As revealed in Fig. 5A, within 6 weeks after the start of administration, the tumor volumes in the EV20-sss-vc/MMAF-treated group were significantly smaller compared with the vehicle-treated group. The growth suppression effect was accompanied by increased survival (Fig. 5B).
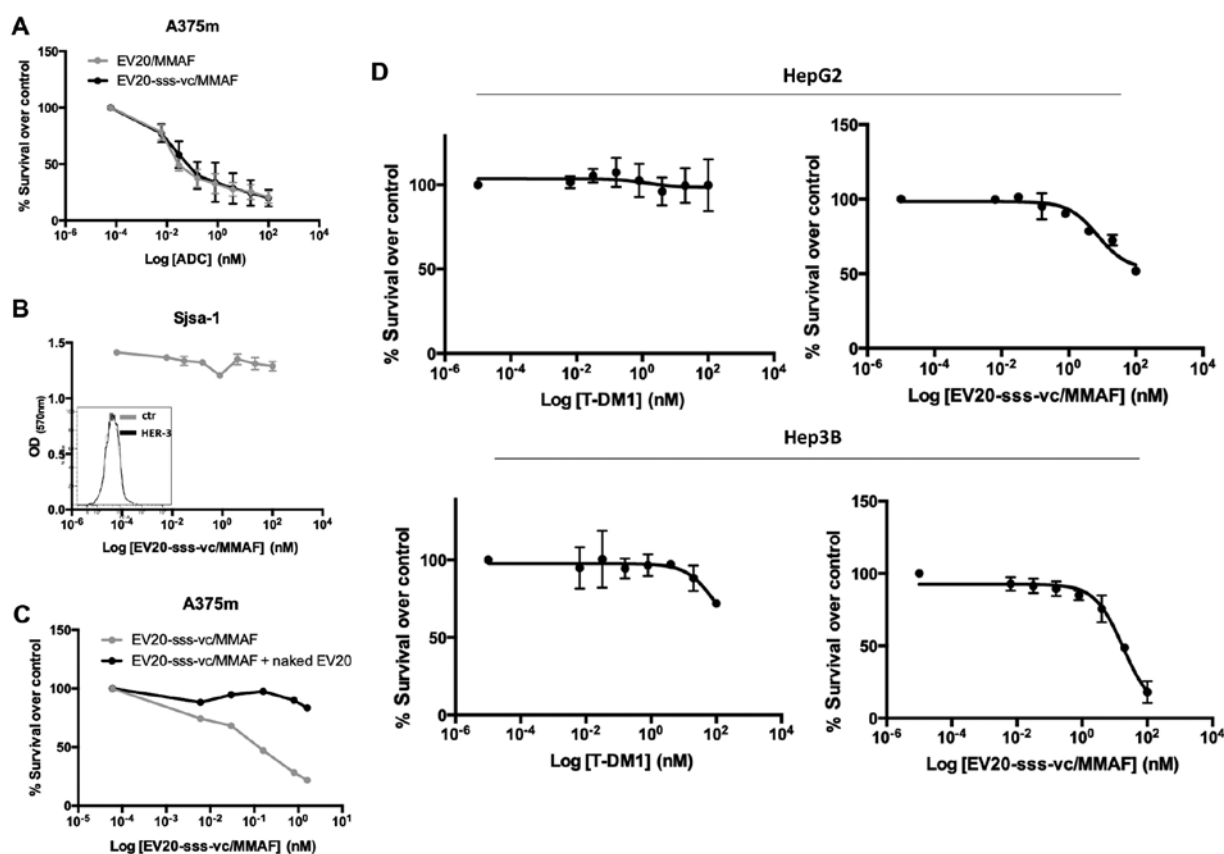
Figure 3. EV20-sss-vc/MMAF cell killing activity is target-dependent and superior to T-DM1. (A) A375m cells were incubated for 120 h with increasing doses of EV20-sss-vc/MMAF or EV20/MMAF ranging between 0.006 nM and 100 nM, and proliferation was evaluated by MTT assay. (B) Cytotoxic response of HER-3 negative SJSA-1 cells to EV20-sss-vc/MMAF treatment (with doses ranging between 0.006 and 100 nM) was evaluated by MTT after 120 h of drug exposure. HER-3 expression by flow cytometric analysis is presented as inset. (C) A375m cells were incubated for 120 h with increasing doses of EV20-sss-vc/MMAF (ranging between 0.006 and 100 nM) alone or with 500-fold molar excess of naked EV20 and proliferation was evaluated by MTT assay. (D) LC cells were exposed for 120 h to increasing doses of T-DM1 or EV20-sss-vc/MMAF (ranging between 0.006 and 100 nM) and proliferation was evaluated by MTT assay as aforementioned. vc, valine-citrulline; MMAF, monomethyl auristatin F; MTT, 3-(4,5-dimethyldiazol-2-yl)-2,5-diphenyl tetrazolium bromide; LC, liver cancer.

Discussion

Primary LC is one of the most common types of cancer worldwide and is currently the third leading cause of cancer-related deaths (1). The therapeutical agent sorafenib, a tyrosine kinase inhibitor, has a limited effect on survival rate, leaving patients with a markedly poor prognosis (8,9).

The number of additional treatment options has recently increased with supplemental FDA approvals of small molecule tyrosine kinase inhibitors (lenvatinib, regorafenib, and cabozantinib) (31), as well as immunotherapies such as immune check point inhibitors (nivolumab and pembrolizumab) (32-35) and the monoclonal IgG1 antibody, ramucirumab (36). These novel therapeutic agents are systemically administered in patients with advanced unresectable tumors either as a single agent or in combination therapy, depending on decisional criteria based on the Barcelona Clinic Liver Cancer (BCLC) staging system, Performance Status (PS) or Child-Pugh system (37). Sorafenib and lenvatinib are used in first-line therapy, whereas regorafenib, cabozantinib and ramucirumab in second-line treatment regimens (31,36).

ADCs represent an emerging class of therapeutics which potentially improve the therapeutic index of cytotoxic agents through a selective targeting mechanism (38). Currently, nine ADCs are already available for treatment but more than 80 different ADCs are in clinical testing and numerous others in preclinical development (38-40).

In the present study, it was revealed that the HER-3 receptor was highly expressed in a panel of patient tumor samples. Moreover, the NRG-1β/HER-3/Akt signalling axis was activated in LC cell lines, thus reinforcing our hypothesis that this receptor represents a suitable target for an ADC. HER-3 is known to potently induce the PI3K/Akt signaling pathway (12), therefore analysis of Akt phosphorylation may be used as a suitable readout for receptor activation. Surprisingly, EV20/MMAF, our previously developed ADC with potent and durable therapeutic activity in melanoma (24) and breast carcinoma (25) displayed only a modest cell killing activity in LC cells.

The reason for the lack of sensitivity of LC cells to EV20/MMAF is presently unknown as these cells express HER-3 and receptor/antibody internalization occurs to the same extent as observed in melanoma and breast cancer cells.

We therefore generated a novel EV20-based ADC with the same cytotoxic payload (i.e. the tubulin inhibitors MMAF) site specifically conjugated to an engineered variant of EV20 (EV20-sss) through a vc cleavable linker. Notably, it was revealed that cell killing induced by EV20-sss-vc/MMAF (DAR ~2 and a cleavable linker) was identical to that induced by EV20/MMAF (DAR ~4.5 and a non-cleavable
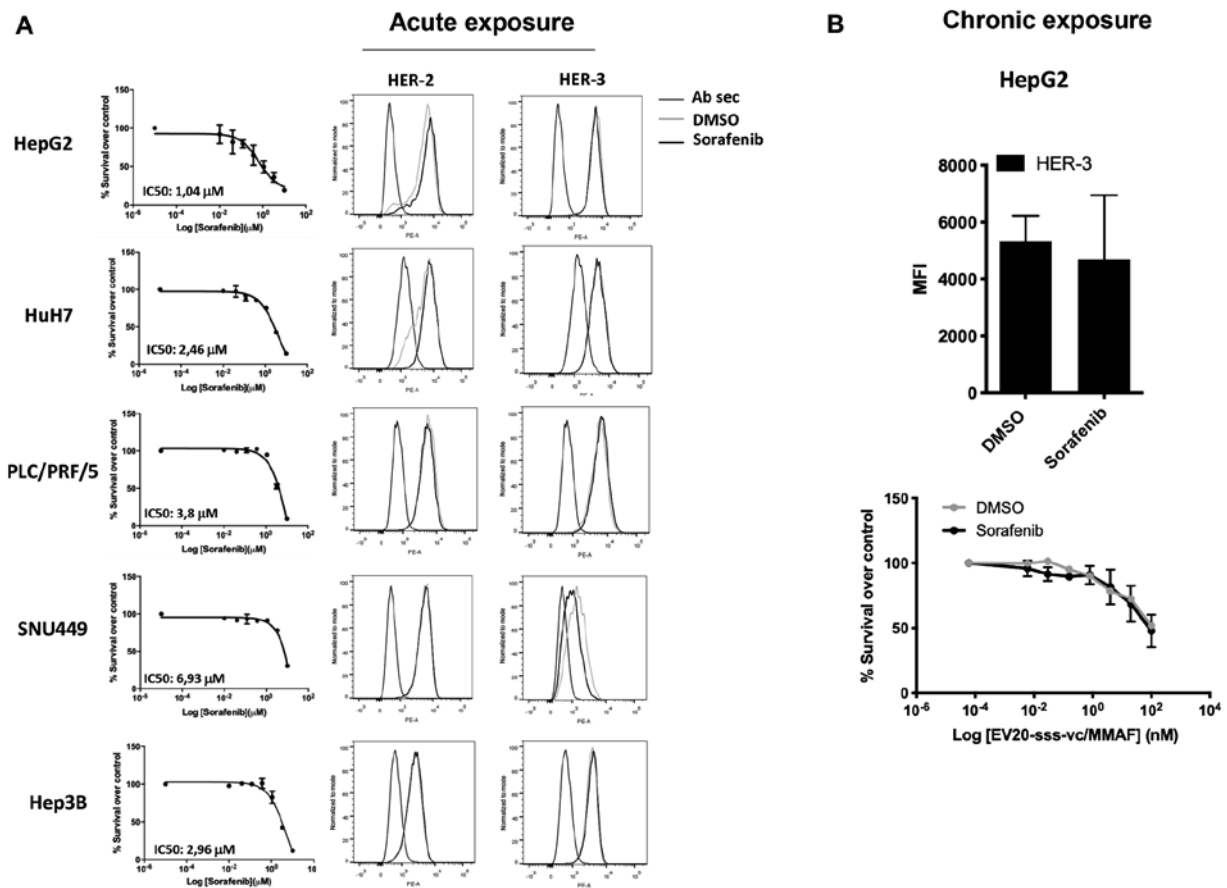
Figure 4. HER-3 expression is not upregulated by sorafenib. (A) LC cells were treated for 24 h with sorafenib (1 μM) or DMSO as control, and then HER-3 and HER-2 surface expression was evaluated by flow cytometry (right panels). The cytotoxic response of LC cells to increasing doses of sorafenib (ranging between 0.001 and 10 μM) was evaluated by MTT after 120 h of treatment. The IC$_{50}$ was calculated with GraphPad Prism 5.0 software and reported (left panels). (B) Surface expression of HER-3 receptor was evaluated by FACS analysis in HepG2 cells grown under chronic treatment of 2 μM of sorafenib. Mean ± SD (n=4) (upper panel). The same cells were analyzed for sensitivity to EV20-sss-vc/MMAF (with doses ranging between 0.006 and 100 nM) by MTT assay after 120 h of treatment (lower panel). LC, liver cancer; MTT, 3-(4,5-dimethyldiazol-2-yl)-2,5-diphenyl tetrazolium bromide; vc, valine-citrulline; MMAF, monomethyl auristatin F; MFI, mean fluorescence intensity; Ab sec, cells stained only with PE-conjugate goat anti-Human Fc (secondary antibody).
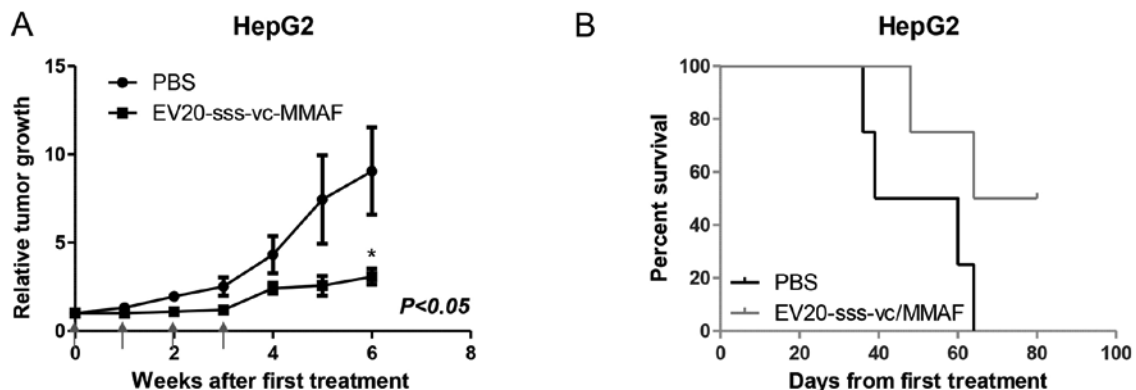

Figure 5. EV20-sss-vc/MMAF therapeutic activity in LC. (A) HepG2 xenografts were established by subcutaneous injection of 5x10^6 cells in a ratio of 1:6 with Matrigel in immunodeficient CD1 mice. When tumors reached a volume of ~150 mm^3, mice were randomized in two groups (n=4) and received four intravenous injections weekly of EV20-sss-vc/MMAF (10 mg/kg) or vehicle alone (PBS). Tumor growth was assessed as described in Materials and methods section and the relative tumor growth was defined as the ratio between the final volume and the initial volume. At the endpoint, mean tumor volumes were 1121±228 and 548±168 mm^3 for control and treated groups, respectively. During the study the maximum volume observed was 1528 mm^3. *P<0.05. (B) Survival was evaluated by Kaplan-Meier curve. vc, valine-citrulline; MMAF, monomethyl auristatin F; LC, liver cancer.

linker) in melanoma cells, but superior in LC cells. This indicated that, at least in LC, the mechanism of cell killing by EV20-sss-vc/MMAF, which is generated with a cleavable linker occurs through cleavage of the cytotoxic payload by the lysosomal cysteine cathepsins rather than via antigen/antibody degradation, which typically occurs when the payload is released in ADCs generated with a non-cleavable linker. However, cell killing activity was not analyzed using

assays which directly reflect tumor proliferation and therefore this could have limited our observations. Studies are ongoing to better elucidate this important aspect. Notably, EV20-sss-vc/MMAF *in vitro* antitumor activity was revealed to be higher compared to that of the clinical approved T-DM1, although receptor expression (HER-3 and HER-2) were similar in LC cells.

It was also investigated whether HER-3 is involved in primary or acquired resistance to sorafenib and we did not observe HER-3 upregulation in response to acute or chronic exposure to sorafenib in HepG2 cells. Accordingly, no increase in cell killing activity was detected in combination treatment, i.e. EV20-sss-vc/MMAF plus sorafenib in comparison to single agents.

Finally, the therapeutic activity of EV20-sss-vc/MMAF at 10 mg/kg in a model of HepG2 xenograft revealed a significant inhibition of tumor growth rate after four doses. A trend for increased survival in treated animals was observed, although this was not significant possibly due to the low number of available mice for this study.

To the best of our knowledge, thus far only another ADC targeting LC has been implemented. This ADC, at the preclinical stage targets glypican-3 (GPC3), a protein found on the surface of LC cells in >70 percent of LC cases (17). The ADC, called hYP7-PC has exhibited potency at picomolar concentrations against a panel of GPC3-positive cancer cell lines (17).

In summary, the present study suggests HER-3 as a potential therapeutic target in LC and fosters further development to increase the activity of EV20-based ADC for LC therapy.

Acknowledgements

Funding

Availability of data and materials

All data generated or analyzed during this study are included in this published article.

Authors' contributions

DDA performed *in vitro* and *in vivo* work. RG performed *in vitro* work and confocal imaging. SP and GDV performed purification of the antibody, conjugation and analytic characterization of the ADC. FD analyzed HER-3 expression in LC tumor samples. GG revised the manuscript critically for important intellectual content. CR supervised the *in vivo* work on the subcutaneous xenografts. LM analyzed the results and revised the manuscript critically for important intellectual content. FG supervised ADC generation, read the manuscript and suggested ideas. VDL analyzed the results and revised the manuscript critically for important intellectual content. SI provided substantial contributions to design of the work and wrote the manuscript. RI provided substantial contributions to the conception of the work and analyzed the results. EC performed and supervised *in vitro* and *in vivo* work and wrote the paper. GS conceived the study, analyzed the results and wrote the manuscript. All the authors read and approved the final manuscript.

Ethics approval and consent to participate

This study was approved by the Local Ethics Committee, Azienda Ospedaliero Universitaria Consorziale Policlinico di Bari (Bari, Italy); protocol no. 254; date of release, February 2012. All patients provided written consent for the use of their specimens for research purposes; none were identifiable. All procedures involving the mice were performed according to the protocol approved by the Institutional Animal Care and Use Committee of the Italian Ministry of Health (Authorization no. 292/2017-PR).

Patient consent for publication

Not applicable.

Competing interests

GS and SI are shareholders of Mediapharma SRL. The other authors have no potential competing interests to disclose.

References

1. Cronin KA, Lake AJ, Scott S, Sherman RL, Noone AM, Howlader N, Henley SJ, Anderson RN, Firth AU, Ma J, *et al*: Annual report to the nation on the status of cancer, part I: National cancer statistics. Cancer 124: 2785-2800, 2018.
2. Jiang BG, Wang N, Huang J, Yang Y, Sun LL, Pan ZY and Zhou WP: Tumor SOCS3 methylation status predicts the treatment response to TACE and prognosis in HCC patients. Oncotarget 8: 28621-28627, 2017.
3. Perini MV, Starkey G, Fink MA, Fink MA, Bhandari R, Muralidharan V, Jones R, Christophi C: From minimal to maximal surgery in the treatment of hepatocarcinoma: A review. World J Hepatol 7: 93-100, 2015.
4. Oda K, Uto H, Mawatari S and Ido A: Clinical features of hepatocellular carcinoma associated with nonalcoholic fatty liver disease: A review of human studies. Clin J Gastroenterol 8: 1-9, 2015.
5. Mizuguchi T, Kawamoto M, Meguro M, Okita K, Ota S, Ishii M, Ueki T, Nishidate T, Kimura Y, Furuhata T, *et al*: Impact of aging on morbidity and mortality after liver resection: A systematic review and meta-analysis. Surg Today 45: 259-270, 2015.
6. Guo XL, Li D, Hu F, Song J, Zhang S, Deng W, Sun K, Zhao Q, Xie X, Song Y, *et al*: Targeting autophagy potentiates chemotherapy-induced apoptosis and proliferation inhibition in hepatocarcinoma cells. Cancer Lett 320: 171-179, 2012.
7. Abou-Alfa GK: Sorafenib use in hepatocellular carcinoma: More questions than answers. Hepatology 60: 15-18, 2014.
8. Zhu AX: Beyond sorafenib: Novel targeted therapies for advanced hepatocellular carcinoma. Expert Opin Investig Drugs 19: 663-672, 2010.
9. Palmer DH: Sorafenib in advanced hepatocellular carcinoma. N Engl J Med 359: 2498, author reply 2498-2499, 2008.

10. Niu L, Liu L, Yang S, Ren J, Lai PBS and Chen GG: New insights into sorafenib resistance in hepatocellular carcinoma: Responsible mechanisms and promising strategies. Biochim Biophys Acta Rev Cancer 1868: 564-570, 2017.
11. Blivet-Van Eggelpoel MJ, Chettouh H, Fartoux L, Aoudjehane L, Barbu V, Rey C, Priam S, Housset C, Rosmorduc O and Desbois-Mouthon C: Epidermal growth factor receptor and HER-3 restrict cell response to sorafenib in hepatocellular carcinoma cells. J Hepatol 57: 108-115, 2012.
12. Mishra R, Patel H, Alanazi S, Yuan L and Garrett JT: HER3 signaling and targeted therapy in cancer. Oncol Rev 12: 355, 2018.
13. Gaborit N, Lindzen M and Yarden Y: Emerging anti-cancer antibodies and combination therapies targeting HER3/ERBB3. Hum Vaccin Immunother 12: 576-592, 2016.
14. Capone E, Prasetyanti PR and Sala G: HER-3: Hub for escape mechanisms. Aging (Albany NY) 7: 899-900, 2015.
15. Jaiswal BS, Kljavin NM, Stawiski EW, Chan E, Parikh C, Durinck S, Chaudhuri S, Pujara K, Guillory J, Edgar KA, *et al*: Oncogenic ERBB3 mutations in human cancers. Cancer Cell 23: 603-617, 2013.
16. Aurisicchio L, Marra E, Roscilli G, Mancini R and Ciliberto G: The promise of anti-ErbB3 monoclonals as new cancer thera-peutics. Oncotarget 3: 744-758, 2012.
17. Fu Y, Urban DJ, Nani RR, Zhang YF, Li N, Fu H, Shah H, Gorka AP, Guha R, Chen L, *et al*: Glypican-3 specific antibody drug conjugates targeting hepatocellular carcinoma. Hepatology 70: 563-576, 2019.
18. Nagayama A, Ellisen LW, Chabner B and Bardia A: Antibody-drug conjugates for the treatment of solid tumors: Clinical experience and latest developments. Target Oncol 12: 719-739, 2017.
19. Moek KL, de Groot DJ, de Vries EG and Fehrmann RS: The antibody-drug conjugate target landscape across a broad range of tumour types. Ann Oncol 28: 3083-3091, 2017.
20. Prasetyanti PR, Capone E, Barcaroli D, D'Agostino D, Volpe S, Benfante A, van Hooff S, Iacobelli V, Rossi C, Iacobelli S, *et al*: ErbB-3 activation by NRG-1beta sustains growth and promotes vemurafenib resistance in BRAF-V600E colon cancer stem cells (CSCs). Oncotarget 6: 16902-16911, 2015.
21. Ghasemi R, Rapposelli IG, Capone E, Rossi C, Lattanzio R, Piantelli M, Sala G and Iacobelli S: Dual targeting of ErbB-2/ErbB-3 results in enhanced antitumor activity in preclinical models of pancreatic cancer. Oncogenesis 3: e117, 2014.
22. Sala G, Rapposelli IG, Ghasemi R, Piccolo E, Traini S, Capone E, Rossi C, Pelliccia A, Di Risio A, D'Egidio M, *et al*: EV20, a novel anti-ErbB-3 humanized antibody, promotes ErbB-3 down-regulation and inhibits tumor growth in vivo. Transl Oncol 6: 676-684, 2013.
23. Sala G, Traini S, D'Egidio M, Vianale G, Rossi C, Piccolo E, Lattanzio R, Piantelli M, Tinari N, Natali PG, *et al*: An ErbB-3 antibody, MP-RM-1, inhibits tumor growth by blocking ligand-dependent and independent activation of ErbB-3/Akt signaling. Oncogene 31: 1275-1286, 2012.
24. Capone E, Lamolinara A, D'Agostino D, Rossi C, De Laurenzi V, Iezzi M, Iacobelli S and Sala G: EV20-mediated delivery of cytotoxic auristatin MMAF exhibits potent therapeutic efficacy in cutaneous melanoma. J Control Release 277: 48-56, 2018.
25. Gandullo-Sanchez L, Capone E, Ocana A, Iacobelli S, Sala G and Pandiella A: HER3 targeting with an antibody-drug conjugate bypasses resistance to anti-HER2 therapies. EMBO Mol Med 12: e11498, 2020.
26. Giansanti F, Capone E, Ponziani S, Piccolo E, Gentile R, Lamolinara A, Di Campli A, Sallese M, Iacobelli V, Cimini A, *et al*: Secreted Gal-3BP is a novel promising target for non-internalizing antibody-drug conjugates. J Control Release 294: 176-184, 2018.
27. Chen R, Hou J, Newman E, Kim Y, Donohue C, Liu X, Thomas SH, Forman SJ and Kane SE: CD30 Downregulation, MMAE resistance, and MDR1 upregulation are all associated with resistance to brentuximab vedotin. Mol Cancer Ther 14: 1376-1384, 2015.
28. Warmann S, Gohring G, Teichmann B, Geerlings H and Fuchs J: MDR1 modulators improve the chemotherapy response of human hepatoblastoma to doxorubicin in vitro. J Pediatr Surg 37: 1579-1584, 2002.
29. Enhanced ERBB3 Signaling promotes resistance in melanoma. Cancer Discov 3: 479, 2013.
30. Chakrabarty A, Sanchez V, Kuba MG, Rinehart C and Arteaga CL: Feedback upregulation of HER3 (ErbB3) expression and activity attenuates antitumor effect of PI3K inhibitors. Proc Natl Acad Sci USA 109: 2718-2723, 2012.
31. Deeks ED: Cabozantinib: A review in advanced hepatocellular carcinoma. Target Oncol 14: 107-113, 2019.
32. Zongyi Y and Xiaowu L: Immunotherapy for hepatocellular carcinoma. Cancer Lett 470: 8-17, 2020.
33. Zhang T, Zhang L, Xu Y, Lu X, Zhao H, Yang H and Sang X: Neoadjuvant therapy and immunotherapy strategies for hepato-cellular carcinoma. Am J Cancer Res 10: 1658-1667, 2020.
34. Llovet JM, Montal R and Villanueva A: Randomized trials and endpoints in advanced HCC: Role of PFS as a surrogate of survival. J Hepatol 70: 1262-1277, 2019.
35. Llovet JM, Montal R, Sia D and Finn RS: Molecular therapies and precision medicine for hepatocellular carcinoma. Nat Rev Clin Oncol 15: 599-616, 2018.
36. De Luca E, Marino D and Di Maio M: Ramucirumab, a second-line option for patients with hepatocellular carcinoma: A review of the evidence. Cancer Manag Res 12: 3721-3729, 2020.
37. Marrero JA, Fontana RJ, Barrat A, Askari F, Conjeevaram HS, Su GL and Lok AS: Prognosis of hepatocellular carcinoma: Comparison of 7 staging systems in an American cohort. Hepatology 41: 707-716, 2005.
38. Ponziani S, Di Vittorio G, Pitari G, Cimini AM, Ardini M, Gentile R, Iacobelli S, Sala G, Capone E, Flavell DJ, *et al*: Antibody-drug conjugates: The new frontier of chemotherapy. Int J Mol Sci 21: 5510, 2020.
39. Coats S, Williams M, Kebble B, Dixit R, Tseng L, Yao NS, Tice DA and Soria JC: Antibody-drug conjugates: Future directions in clinical and translational strategies to improve the therapeutic index. Clin Cancer Res 25: 5441-5448, 2019.
40. Birrer MJ, Moore KN, Betella I and Bates RC: Antibody-drug conjugate-based therapeutics: State of the science. J Natl Cancer Inst 111: 538-549, 2019.